J. Membrane Biol. 31, 383–417 (1977)

Ionic Selectivity, Saturation and Block in Gramicidin A Channels:

I. Theory for the Electrical Properties of Ion Selective Channels Having Two Pairs of Binding Sites and Multiple Conductance States

John Sandblom, George Eisenman, and Erwin Neher

Department of Physiology and Medical Biophysics, University of Uppsala, Sweden;
Department of Physiology, University of California Medical School, Los Angeles, California; and
Max-Planck-Institut für Biophysikalische Chemie, Göttingen, German Federal Republic

Received 19 July 1976; revised 4 November 1976

Summary. A model for the gramicidin A channel is proposed which extends existing models by adding a specific cationic binding site at each entrance to the channel. The binding of ions to these outer channel sites is assumed to shift the energy levels of the inner sites and barriers and thereby alter the channel conductance. The resulting properties are analyzed theoretically for the simplest case of two inner sites and a single energy barrier. This four-site model (two outer and two inner) predicts that the membrane potential at zero current (U_0) should be described by a Goldman-Hodgkin-Katz equation with concentration-dependent permeability ratios. The coefficients of the concentration-dependent terms are shown to be related to the peak energy shifts of the barrier and to the binding constants of the outer sites. The theory also predicts the channel conductance in symmetrical solutions to exhibit three limiting behaviors, from which the properties of the outer and inner sites can be characterized. In two-cation symmetrical mixtures the conductance as a function of mole fraction is shown to have a minimum, and the related phenomenon of inhibition and block exerted by one ion on the other is explained explicitly by the theory. These various phenomena, having ion interactions in a multiply occupied channel as a common physical basis, are all related (by the theory) through a set of measurable parameters describing the properties of the system.

Since the discovery of substances which can form ionic channels in lipid bilayer membranes, a number of theoretical treatments have been developed to describe the transport of ions through these channels. By considering the ions to pass through a series of equilibrium positions (sites) and applying the rate theory analysis to such models, it has been possible to explain several effects of channel-forming compounds on the permeability properties of bilayer membranes. These include saturation effects, i.e., the attainment of a maximum conductance or transport rate as the concentrations in the bathing solutions increase (Hladky & Harris,

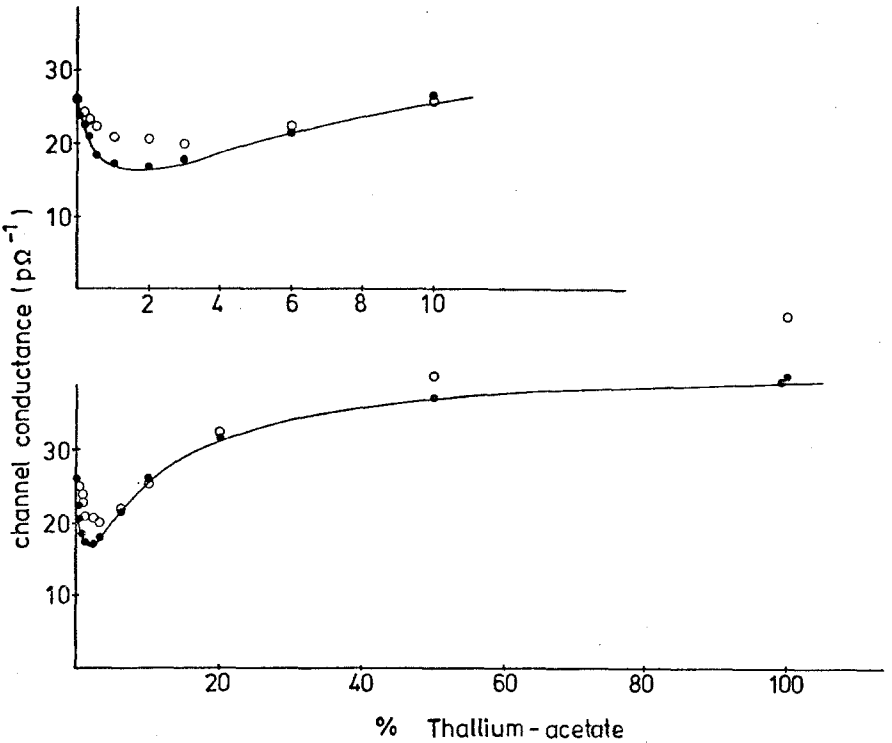

Fig. 1. Conductance of single gramicidin A channels as mole fractions of Tl^+ at 1 M total concentration of TlAc – NaAc mixtures of equal compositions on both sides of the membrane. Filled circles give the zero current conductance, open circles the conductance measured at ± 100 mV. The upper part expands the low Tl^+ concentration region around the conductance minimum. Replotted after Neher (1975)

1967; Myers & Haydon, 1972; Läuger, 1973), as well as blocking at the highest concentrations (Hladky, 1972, 1974). They also include coupling between different ions as a result of single file diffusion (Heckmann & Vollmerhaus, 1970; Heckmann, 1972) and certain nonlinearities in the I–V curves (Heckmann, Lindemann & Schnakenberg, 1972; Läuger, 1973).

A recent observation, which gives an additional clue to the mechanism of transport through these channels, has been reported by Neher (1975) for gramicidin A in the presence of sodium and thallium, namely, the appearance of a minimum in the conductance curve as the mole fractions of the ions in the external solutions are varied (*see* Fig. 1). The phenomenon indicates the presence of interactions between ions in the channel as a result of which the channel properties are altered by changes in solution compositions. Although such a conclusion seems to contradict the argument (Hladky & Haydon, 1972, Läuger, 1973) that the electroneutral but

cation selective gramicidin A channel is unlikely to contain more than one ion for electrostatic reasons, it is conceivable that cations may approach and bind to the entrance of an already occupied channel, thereby modifying the channel properties without actually entering the channel, and leave the anions behind. Indeed, Hladky (1972) has already considered the blocking effects of a second ion in his two-site model for the channel.

By assuming the existence of such additional outer binding sites at each side of the membrane, a model has been developed to explain the minimum in the conductance curve, observed independently by Neher (1975) and by Andersen (1975). Apart from being able to account for the minimum conductance phenomenon, however, the model also predicts the ionic permeability ratios to be concentration dependent as a result of ionic interactions in the channel. This prediction is considered to be an important criterion for the existence of multiple sites, and a set of experiments designed to test the model (Eisenman, Sandblom & Neher)[1] have not only verified the existence of concentration-dependent permeability ratios for the gramicidin A channel but also confirmed the form of the derived expressions for the permeability ratios.

The model has briefly been described in two preliminary reports (Eisenman, Sandblom & Neher, 1976*a*; Eisenman, Sandblom & Neher, 1976*b*), and a more detailed treatment, explaining several of the observed properties of channels associated with binding and ionic interactions, will be given in this paper.

Model

The recently accumulated data on the structure of gramicidin A seems to indicate that the molecules on entering a lipid bilayer membrane form dimers (Urry, Goodall, Glickson & Mayers, 1971; Veatch, Fossel & Blout, 1974), possibly linked together by hydrogen bonds in the middle of the membrane (Urry, 1972*a*, Urry, 1972*b*). It is therefore reasonable, following Läuger (1973) and Hladky (1972, 1974), to represent the membrane as a two-compartment system, each side of the membrane constituting one compartment. The modification introduced here is to divide each compartment into two separate regions or binding sites for ions (*see* Fig. 2), thereby adding two additional possible binding sites to Hladky's model.

1 Eisenman, G., Sandblom, J., Neher, E. 1976. Ionic Selectivity, binding, and block in the gramicidin A channel: II. Membrane potentials in ionic mixtures and concentration-dependent permeability ratios for K^+ and Tl^+ *(in preparation)*.

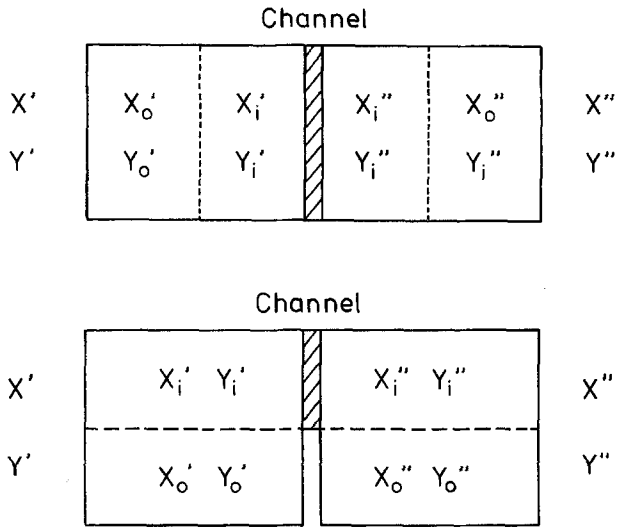

Fig. 2. Four-compartment model of gramicidin A channel showing the locations of the sites relative to one another. Each site is represented by a compartment, which can contain either the cation *X* or *Y*. (*a*) shows a longitudinal arrangement and (*b*) a radial rearrangement of outer (*o*) and inner (*i*) sites in the channel. Note that in each case an ion can pass the internal barrier only from the inner sites

The physical situation corresponding to this picture could be that the two types of sites, *outer* and *inner*, are located in different places along the channel as shown in Fig. 2*a*, i.e., a series arrangement of sites.

The other alternative, shown schematically in Fig. 2*b*, is a parallel or radial arrangement of sites where the outer sites are located near the wall of the channel and the inner sites in interstitial positions next to the outer sites. In either alternative an ion can pass from one inner site to the opposite inner site by overcoming an energy barrier (or a series of energy barriers), shown in Fig. 2 by cross-hatching.

The interesting set of properties associated with this model appear not only as a result of allowing the channel to be occupied by several ions at the same time but also by taking into account the change in channel properties induced by ion binding to the sites. A particular set of channel properties (conductance state) expressed in terms of rate constants (barrier heights) and binding constants (energy wells) for the ions will then correspond to each configuration of ion occupancy (so called channel state).

The highest degree of occupancy (4 ions in this model) is expected to be energetically unfavorable for electrostatic reasons, and should therefore become significant only at very high concentrations. In a state where all sites are occupied, the channel conductance is also expected to be

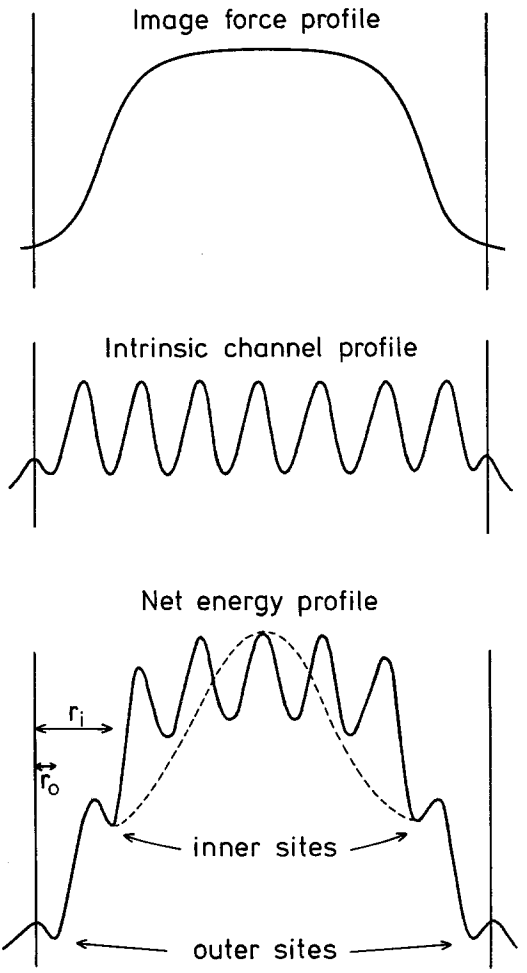

Fig. 3. Schematic representation of the energy profile of a channel. The net profile is obtained as a sum of the image force profile and the intrinsic channel profile arising from specific ion channel interactions. The resulting energy profile can be approximated by 2 binding sites near each membrane surface and a single internal barrier (broken line) in the center of the membrane

completely blocked, a tendency which is observed experimentally for several cations at high concentrations (Myers & Haydon, 1972; Hladky, 1972, 1974). It is therefore necessary to include the possibilities of 4-ion occupancies in the theoretical treatment.

An energetic basis for a 4-ion occupied multi-site channel is suggested in Fig. 3. The net energy profile for the channel (lower part) is composed of the image-force profile (upper part) and an intrinsic channel profile (middle part). An ion occupying one of the outer sites is assumed to be

Table 1. Experimental values for TlCl and KCl in single channels of Gramicidin A [Neher, Eisenman & Sandblom, 1976 *(in preparation)*][a]

Binding constants	Maximal limiting conductances	Permeability coefficients (potential data)
K^o_{Tl} 3600 M^{-1}	G^o_{Tl} 0.53 pS	α 3.5
K^o_K 260 M^{-1}	G^o_K 2.12 pS	β_{Tl} 1000 M^{-1}
K^h_{Tl} 45 M^{-1}	G^h_{Tl} 10.44 pS	β_K 80 M^{-1}
K^h_K 2.9 M^{-1}	G^h_K 71.5 pS	γ_{Tl} 500 M^{-1}
K^∞_{Tl} 0 M^{-1}		γ_K 80 M^{-1}
K^∞_K 0.22 M^{-1}		
$\frac{G^o_{Tl} K^o_{Tl}}{G^o_K K^o_K} = 3.5$		$(=\alpha)$
$\frac{1}{2} K^o_{Tl} \left(\frac{G^h_{Tl} K^h_{Tl}}{G^o_{Tl} K^o_{Tl}}\right)^{\frac{1}{2}} = 900\ M^{-1}$		$(=\beta_{Tl})$
$\frac{1}{2} K^o_K \left(\frac{G^h_K K^h_K}{G^o_K K^o_K}\right)^{\frac{1}{2}} = 80\ M^{-1}$		$(=\gamma_K)$

[a] The experimental values are essentially obtained from the limiting behavior corresponding to Eq. (34) for the potential data and Eqs. (41), (43) and (45) for conductance data. The superscripts refer to the limits of low concentrations (o), high concentrations (h), and concentrations tending towards infinity (∞).

sufficiently near the aqueous surface to allow the nearest inner site to be occupied by another cation. If, in addition, the energy levels of the first inner sites are well below the top of the image-force profile the ions will spend relatively little time in the energy wells near the center of the membrane compared to the time spent in the first inner sites. It is therefore justified to incorporate all the inner barriers into a single central barrier.

An estimate of the respective locations of the outer and inner sites which is consistent with coulombic interactions between ions occupying two neighboring outer and inner sites can be made using experimental data for the binding constants. According to experimental data for potassium conductance (*see* Table 1), there is a reduction in binding constant by a factor of 1000 in loading the channel with a single ion as opposed to loading it with 4 ions. The reduction in binding constant per added ion is therefore approximately 10, which corresponds to about 2.5 kT. The repulsive interaction energy between two cations near a conducting planar surface is derived using image charges, i.e.,

$$W = \frac{e^2 r_o}{2\pi\varepsilon(r_i^2 - r_o^2)}$$

where r_o is the distance from the aqueous solution to the outer site and r_i the corresponding distance to the inner site (*see* Fig. 3). An estimated distance between the sites of the gramicidin A channel is 10 Å (Läuger, 1973). If the relative dielectric constant is set equal to 10, the value of r_o is about 5 Å. A 4-site model is therefore physically reasonable if the outer sites are located very near the surfaces, presumably at the mouths of the channel.

In this paper it will also be assumed that the rate of exchange of ions between the external solutions and the outer sites as well as that between the sites of each compartment is rapid compared to the passage of ions through the channel (across the central barrier). This assumption implies that the outer sites as well as the inner sites are in equilibrium with the external solutions, and hence the sequence of loading the sites depends only on their respective energy levels which also makes the two alternative arrangements of sites in Fig. 2 indistinguishable.

It also eliminates the particular kind of flux coupling called "single filing" which is characteristic of narrow channels in which neighboring ions are unable to exchange their positions (Heckmann & Vollmerhaus, 1970; Heckmann, 1972). If the model is extended to include several interior barriers, the "single filing" phenomenon will still be absent as long as the inner part of the channel is allowed to contain only one ion. This extension of the model corresponds in principle to previous treatments of singly occupied pores (Heckman *et al.*, 1972; Läuger, 1973), except for the addition of a pair of outer sites which can modify (modulate) the channel properties in their occupied states. Extensions of this kind should have considerable interest not only for ionic channels formed by gramicidin A and other ionophores but also for biological membranes, in view of the recent findings by Hille (1975*a*; 1975*b*) and by Cahalan and Begenisich (1975; 1976) suggesting that ions can modify the transport properties of a channel by attaching to specific binding sites. The extension of the present model to multi-site channels and the possible biological implications will be considered in the discussion.

Multiple Occupancy and Concentration Dependent Permeabilities

In the theoretical part of this paper, the properties of the model will be analyzed in terms of expressions for conductances and permeability ratios. It is immediately deduced, however, that the ionic permeability must be concentration dependent since the states of occupancy depend on external solution concentrations. For instance, if an ion X is passing

through the channel when an ion Y is occupying the outer site at the side of the channel labelled prime, the probability of a transfer of X in that particular state is proportional to the concentration, C'_y, of the ion Y in the external solution. Consequently the permeability of X must be proportional to the sum of the three probabilities corresponding to the three different possible states of occupancy of the outer site, since they form mutually excluding events, i.e., $P_x = \alpha_x(1+\beta_x C'_x+\beta_y C'_y)$. Since the three states can occur jointly with the same three states on the opposite side of the channel, the expected expression for the permeability of X in the presence of Y is given by

$$P_x = \alpha_x(1+\beta_x C'_x+\beta_y C'_y)(1+\beta_x C''_x+\beta_y C''_y). \tag{1}$$

Eq. (1), which has been derived here by probabilistic arguments, will be derived more rigorously from a physical theory by which the coefficients can be related to shifts in the energy barrier peaks.

Anion Permeability

The model also allows for the passage of anions, although the anion permeability of the gramicidin A channel, according to Myers and Haydon (1972), is practically negligible. It is therefore assumed that the channel sites are exclusively cation binding, although electroneutral, an assumption which is also consistent with the structure proposed by Urry *et al.* (1971), Urry (1972*a*, 1972*b*) and Veatch *et al.* (1974), in which carbonyl groups are facing the interior of the channel and presumably form part of the cationic binding sites. The resulting large electrostatic barrier to anions can, however, be sufficiently reduced by the presence of cations in the channel to enable the anions to enter the channel. There is some experimental evidence to support this assumption which can be deduced from different observations.

One such observation concerns the anion permeability which has been shown to occur in the presence of high concentrations of thallous ion where the outer sites are expected to be loaded with Tl^+ (Eisenman *et al.*, 1976*b*).[2]

Theory

Having outlined the model and the underlying physical assumptions, the properties associated with the system can be analyzed in terms of theoretical expressions for the transport of ions through the channel.

2 *Ibid.*

Formally the model can be represented as a channel with two cationic sites at each side of the membrane each in equilibrium with the adjacent external solutions. The two sides are separated by an energy barrier, the height of which will in general depend on the "state" of the channel, i.e., the particular configuration of occupied and unoccupied sites. Having formulated this model of the gramicidin A channel the next step is to derive the equations describing the transport of ions through this system in the various channel states. Hladky (1972) has previously considered the case for one cationic site at each side of the membrane.

(a) Channel States

If the symbol S is used to denote the empty channel and the symbol X is used to denote a particular cation, it is possible to combine these letters to designate a particular channel configuration, for which the term channel state will be used. The combination $X'S$ is therefore the symbol for the condition in which the channel is occupied by ion X in compartment $'$ (not specifying which site) in a channel which is otherwise empty. The process by which the ion X enters a site on the left side may therefore be represented as: $X'+S \rightleftharpoons X'_oS \rightleftharpoons X'_iS$, where the subscripts o and i refer to outer and inner sites respectively.

The formation of other channel states are obtained in exactly the same way, for instance with an additional ion Y:

$$Y''+X'S \rightleftharpoons Y''_oX'_oS \rightleftharpoons Y''_iX'_oS \rightleftharpoons Y''_oX'_iS, \tag{2}$$

which describes the process by which an ion Y enters the right compartment from the aqueous solution on side $''$ when the channel is already in one of the states $X'S$. As illustrated by the equation, the channel configuration represented by $Y''X'S$ consists of 3 possible states, the probabilities of which depend on the respective free energy levels. In the case of two ions, each site can have 3 different occupancy alternatives: either unoccupied, or occupied by X or Y. Therefore, the total number of channel states which can be formed with four sites and two cations are $3^4=81$.

In the following, the notation N_j will be assigned to the fraction of time during which the channel will be in state j. Therefore,

$$\sum_{j=1}^{81} N_j = 1. \tag{3}$$

80 of the state parameters N_j will be determined by exchange equilibria of the type given by Eq. (2) whereas the remaining state parameter N_s, describing the fraction of time during which the channel is completely empty, is obtained from Eq. (3).

(b) Transitions

Equations of the type exemplified by Eq. (2) describe only the exchange processes between the aqueous solutions and the two channel compartments. The transport of ions across the internal energy barrier must be given in another set of equations, describing the transitions between interior regions, e.g.: $X_i' S \rightleftharpoons X_i'' S$. The total number of such possible transitions are 12, namely:

$$X_i' S \rightleftharpoons X_i'' S \tag{4}$$

$$Y_i' S \rightleftharpoons Y_i'' S \tag{5}$$

$$X_o' X_i' S \rightleftharpoons X_i'' X_o' S \qquad X_o'' X_i'' S \rightleftharpoons X_i' X_o'' S \tag{6a, b}$$

$$Y_o' Y_i' S \rightleftharpoons Y_i'' Y_o' S \qquad Y_o'' Y_i'' S \rightleftharpoons Y_i' Y_o'' S \tag{7a, b}$$

$$Y_o' X_i' S \rightleftharpoons X_i'' Y_o' S \qquad Y_o'' X_i'' S \rightleftharpoons X_i' Y_o'' S \tag{8a, b}$$

$$X_o' Y_i' S \rightleftharpoons Y_i'' X_o' S \qquad X_o'' Y_i'' S \rightleftharpoons Y_i' X_o'' S \tag{9a, b}$$

$$X_o' X_o'' X_i' S \rightleftharpoons X_i'' X_o' X_o'' S \tag{10}$$

$$Y_o' Y_o'' Y_i' S \rightleftharpoons Y_i'' Y_o' Y_o'' S \tag{11}$$

$$Y_o' Y_o'' X_i' S \rightleftharpoons X_i'' Y_o' Y_o'' S \tag{12}$$

$$X_o' X_o'' Y_i' S \rightleftharpoons Y_i'' X_o' X_o'' S \tag{13}$$

$$Y_o'' X_o' X_i'' S \rightleftharpoons X_i' X_o' Y_o'' S \qquad Y_o' X_o'' X_i' S \rightleftharpoons X_i'' X_o'' Y_o' S \tag{14a, b}$$

$$X_o'' Y_o' Y_i'' S \rightleftharpoons Y_i' Y_o' X_o'' S \qquad X_o' Y_o'' Y_i' S \rightleftharpoons Y_i'' Y_o'' X_o' S. \tag{15a, b}$$

The number of transitions is relatively small compared to the number of possible states due to the fact that only those states having an ion in one inner site while the other is vacant provide the proper conditions for the transfer of an ion across the central barrier.

Additional states would provide the proper conditions for transitions if these could take place by means of ion displacements (knock-on, knock-off) such as those considered by Hladky and Harris (1967). Then it would not be necessary to require an inner site to be vacant in order for transi-

tions to occur. Therefore, the states consisting of full channel occupancy would allow transitions involving the displacements of adjacent ions from their sites, e.g.,

$$X'_o X''_o X'_i X''_i \rightleftharpoons X'_o X''_o X''_i + X'';$$

$$X' + X'_o X''_o X'_i \rightleftharpoons X'_o X''_o X'_i X''_i.$$

However, experimental evidence (Myers and Haydon, 1972) suggests that the activation energy for such displacement transitions is very high, since the conductance at high concentrations (where the channel becomes saturated) shows a tendency to decrease. Displacement transitions will therefore be neglected in the following treatment.

The 12 transition reactions together with the 81 exchange equilibria completes the formal description of the model.

(c) Boundary Equilibria

It has been assumed that the exchange reactions across the boundaries [exemplified by Eq. (2)] are rapid compared to the interior transition rates. This means that the variables N_j can be obtained from the set of equilibrium conditions corresponding to the respective states. For instance, the equilibrium condition corresponding to the state $Y''_o X'_o S$, formed according to Eq. (2), is written

$$N_{y''_o x'_o s} = k^{x'_o}_{y''_o} \cdot C''_y \cdot N_{x'_o s} = k^{x'_o}_{y''_o} \cdot C''_y \cdot k_{x'_o} \cdot C'_x \cdot N_s. \tag{16}$$

The symbols k represent binding constants. The *subscript* of a particular binding constant indicates which ion binds to a particular site, and the *superscript* indicates the prebinding condition, i.e., the state in which the channel finds itself when the indicated ion loads onto the indicated site.

Eq. (16), relating $N_{y''_o x's}$ to N_s, is based on the equilibria of two sequential bimolecular reactions. However, the state variable $N_{y''_o x'_o s}$ can also be related to N_s through a single trimolecular reaction.

$$N_{y''_o x'_o s} = k_{y''_o x'_o} C''_y C'_x N_s. \tag{17}$$

It follows immediately that

$$k_{y''_o x'_o} = k^{x'_o}_{y''_o} k_{x'_o} = k^{y''_o}_{x'_o} k_{y''_o}. \tag{18}$$

The remaining state variables are obtained from their corresponding state equations in analogy to Eq. (16) and each state equation defines a new binding constant. Consequently there are 80 independent binding constants describing the binding properties of the sites of this model.

If, however, the symmetry of the two channel halves is taken into account, the number of independent binding constants is reduced to

$$\frac{\text{number of states} + \text{number of symmetrical states}}{2} - \text{empty state}$$

$$= \frac{81+9}{2} - 1 = 44.$$

In reducing the number of independent binding constants, it is advantageous to use a notation which is independent of the membrane side. Inserting a colon in the super- and subscripts to denote the location of the barrier, the explicit expression for N_s, obtained from Eq. (3), is written in terms of the 44 independent binding constants,

$$\begin{aligned}
1/N_s = {} & 1 + (k_{x_i:} + k_{x_o:})(C'_x + C''_x) + (k_{y_i:} + k_{y_o:})(C'_y + C''_y) \\
& + k_{x_o x_i:}(C'^2_x + C''^2_x) + k_{y_o y_i:}(C'^2_y + C''^2_y) \\
& + (k_{x_o:x_o} + 2k_{x_o:x_i} + k_{x_i:x_i})\, C'_x\, C''_x \\
& + (k_{y_o:y_o} + 2k_{y_o:y_i} + k_{y_i:y_i})\, C'_y\, C''_y + (k_{x_o y_i:} + k_{y_o x_i:})(C'_x\, C'_y + C''_x\, C''_y) \\
& + (k_{x_o:y_i} + k_{x_o:y_o} + k_{x_i:y_o} + k_{x_i:y_i})(C'_x\, C''_y + C''_x\, C'_y) \\
& + (k_{x_o x_i:x_o} + k_{x_o x_i:x_i})\, C'_x\, C''_x (C'_x + C''_x) \\
& + (k_{y_o y_i:y_o} + k_{y_o y_i:y_i})\, C'_y\, C''_y (C'_y + C''_y) \\
& + (k_{x_o:y_i y_o} + k_{x_i:y_i y_o})(C'_x\, C''^2_y + C''_x\, C'^2_y) \\
& + (k_{y_o:x_i x_o} + k_{y_i:x_i x_o})(C'_y\, C''^2_x + C''_y\, C'^2_x) \\
& + (k_{x_o:y_i x_o} + k_{x_o:x_i y_o} + k_{x_i:y_i x_o} + k_{x_i:x_i y_o})\, C'_x\, C''_x (C'_y + C''_y) \\
& + (k_{y_o:y_i x_o} + k_{y_o:x_i y_o} + k_{y_i:y_i x_o} + k_{y_i:x_i y_o})\, C'_y\, C''_y (C'_x + C''_x) \\
& + k_{x_o x_i:x_i x_o}\, C'^2_x\, C''^2_x + k_{y_o y_i:y_i y_o}\, C'^2_y\, C''^2_y \\
& + (k_{y_o x_i:x_i x_o} + k_{x_o y_i:x_i y_o})\, C'_x\, C''_x (C'_x\, C''_y + C''_x\, C'_y) \\
& + (k_{y_o x_i:y_i y_o} + k_{x_o y_i:y_i y_o})\, C'_y\, C''_y (C'_x\, C''_y + C''_x\, C'_y) \\
& + k_{y_o y_i:x_i x_o}(C'^2_x\, C''^2_y + C''^2_x\, C'^2_y) \\
& + (k_{x_o y_i:y_i x_o} + 2k_{x_o y_i:x_i y_o} + k_{y_o x_i:x_i y_o})\, C'_x\, C'_y\, C''_x\, C''_y .
\end{aligned} \tag{19}$$

Eq. (19) is seen to contain 81 terms and 44 independent constants as mentioned above. From a practical point of view, however, it is too cumbersome to retain all the constants and by making reasonable assumptions it is possible to reduce the number considerably, as will be shown later.

(d) Rate Equations

The rate equations for the set of transitions (4)–(15) are obtained from rate theory (Eyring, Lumry & Woodbury, 1949; Woodbury, 1971), and the total membrane potential will thereby be assumed to be equal to the potential drop across the central barrier between the inner sites.

Since Eqs. (6)–(9), (14) and (15) involve transitions which are asymmetric, in other words the energy barrier is different in the two directions, there are in principle 18 rate constants corresponding to Eqs. (4)–(15). However, the condition of microscopic reversibility applied to these equations will reduce the number of independent rate constants to 12. The proof of this is given below for Eq. (6). The transition rate corresponding to Eq. (6*a*) is given by:

$$\begin{aligned} i_{x_i:}^{x_o:} &= z_x\, e\, v_{x_i:}^{x_o:} \cdot N_{x_i' x_o'}\, e^{\frac{z_x FU}{2RT}} - z_x\, e\, v_{:x_i}^{x_o:} \cdot N_{x_i'' x_o'}\, e^{-\frac{z_x FU}{2RT}} \\ &= z_x\, e\, N_s\, v_{x_i:}^{x_o:} \cdot k_{x_o x_i:}\, C_x'\, C_x'\, e^{\frac{z_x FU}{2RT}} - z_x\, e\, N_s\, v_{:x_i}^{x_o:} \cdot k_{x_o x_i}\, C_x''\, C_x'\, e^{-\frac{z_x FU}{2RT}}, \end{aligned} \tag{20}$$

where $i_{x_i:}^{x_o:}$ is the current produced by the transitions (6*a*), $v_{x_i:}^{x_o:}$ the rate constant (jump frequency for a jump from state $X_i' X_o'$ to state $X_i'' X_o'$) and $v_{x_i:}^{:x_o}$ the rate constant for a jump in the opposite direction ($X_i'' X_o'$ to $X_i' X_o'$). e is the electronic charge. The principle of microscopic reversibility applied to a reversible transfer of X from one solution to the other, the rate of which is equal in both direction under symmetrical solution conditions, gives:

$$\begin{aligned} &\vec{k}'(\text{solution}\,|\,\text{inner site}) \cdot \vec{k}\,(\text{inner site}\,|\,\text{inner site}) \cdot \vec{k}''(\text{inner site}\,|\,\text{solution}) \\ &= \overleftarrow{k}'(\text{inner site}\,|\,\text{solution}) \cdot \overleftarrow{k}\,(\text{inner site}\,|\,\text{inner site}) \cdot \overleftarrow{k}''(\text{solution}\,|\,\text{inner site}) \end{aligned} \tag{21}$$

where

$$\begin{aligned} &\vec{k}\ \ (\text{inner site}\,|\,\text{inner site}) = v_{x_i:}^{x_o:} \\ &\overleftarrow{k}\ \ (\text{inner site}\,|\,\text{inner site}) = v_{:x_i}^{x_o:} \\ &\vec{k}'\ (\text{solution}\,|\,\text{inner site})/\overleftarrow{k}'(\text{inner site}\,|\,\text{solution}) = k_{x_o x_i:} \\ &\overleftarrow{k}''\ (\text{solution}\,|\,\text{inner site})/\vec{k}''\ (\text{inner site}\,|\,\text{solution}) = k_{x_o: x_i}. \end{aligned}$$

Taking into account the identified rate constants and inserting Eq. (21) in Eq. (20) gives:

$$i_{x_i:}^{x_o:} = z_x\, e\, N_s\, v_{x_i:}^{x_o:} \cdot k_{x_o x_i:}\, C_x''\left(C_x'\, e^{\frac{z_x FU}{2RT}} - C_x''\, e^{-\frac{z_x FU}{2RT}}\right). \tag{22}$$

If the same procedure is then applied to Eq. (6*b*) a similar equation is obtained:

$$i_{:x_i}^{x_o:} = z_x\, e\, N_s\, v_{x_i:}^{x_o:} \cdot k_{x_o x_i:}\, C_x'\left(C_x'\, e^{\frac{z_x FU}{2RT}} - C_x''\, e^{-\frac{z_x FU}{2RT}}\right). \tag{23}$$

Adding Eqs. (22) and (23) therefore gives the net contribution to the current produced by the transitions described by Eq. (6):

$$i_{x_i}^{x_o} = z_x\, e\, N_s \cdot v_{x_i:}^{x_o:} \cdot k_{x_o x_i:}(C'_x + C''_x)\left(C'_x\, e^{\frac{z_x FU}{2RT}} - C''_x\, e^{-\frac{z_x FU}{2RT}}\right). \tag{24}$$

The proof just given essentially implies that an ion X sees the same energy peak from either side of the membrane.

Flux Equations

The total current I_x of ion X is obtained by adding the rate equations corresponding to the X-transitions (4, 6, 8, 10, 12 and 14), where the principle of microscopic reversibility is used to reduce the rate constants in Eqs. (6), (8) and (14). A similar procedure is used to obtain the total current I_y of ion Y. The final equations for the currents of the cation species X and Y therefore take the simple form

$$I_x = z_x\, e\, N_s\, P_x\left(C'_x\, e^{\frac{z_x FU}{2RT}} - C''_x\, e^{-\frac{z_x FU}{2RT}}\right) \tag{25a}$$

$$I_y = z_y\, e\, N_s\, P_y\left(C'_y\, e^{\frac{z_y FU}{2RT}} - C''_y\, e^{-\frac{z_y FU}{2RT}}\right), \tag{25b}$$

where P_x and P_y, the permeabilities of X and Y, are conveniently defined as:

$$\begin{aligned} P_x = {} & v_{x_i:} \cdot k_{x_i:} + v_{x_i:}^{x_o:} \cdot k_{x_o x_i:}(C'_x + C''_x) + v_{x_i:}^{y_o:} \cdot k_{y_o x_i:}(C'_y + C''_y) \\ & + v_{x_i:}^{x_o:x_o} \cdot k_{x_o x_i:x_o}\, C'_x\, C''_x + v_{x_i:}^{y_o:y_o} \cdot k_{y_o x_i:y_o}\, C'_y\, C''_y \\ & + v_{x_i:}^{y_o:x_o} \cdot k_{y_o x_i:x_o}(C'_x\, C''_y + C''_x\, C'_y), \end{aligned} \tag{26a}$$

$$\begin{aligned} P_y = {} & v_{y_i:} \cdot k_{y_i:} + v_{y_i:}^{y_o:} \cdot k_{y_o y_i:}(C'_y + C''_y) + v_{y_i:}^{x_o:} \cdot k_{x_o y_i:}(C'_x + C''_x) \\ & + v_{y_i:}^{y_o:y_o} \cdot k_{y_o y_i:y_o}\, C'_y\, C''_y + v_{y_i:}^{x_o:x_o} \cdot k_{x_o y_i:x_o}\, C'_x\, C''_x \\ & + v_{x_i:}^{y_o:x_o} \cdot k_{y_o y_i:x_o}(C'_x\, C''_y + C''_x\, C'_y). \end{aligned} \tag{26b}$$

The anion current is derived directly by applying rate theory to the anion transitions, which can occur in one or several of the 81 cationic states. The expression for the anion current is therefore given by

$$I_A = z_A\, e\, N_s\, P_A\left(C'_A\, e^{\frac{z_A FU}{2RT}} - C''_A\, e^{-\frac{z_A FU}{2RT}}\right), \tag{27}$$

where

$$P_A = \sum_{j=1}^{81} v_A^j\, N_j / N_s. \tag{28}$$

The rate constant v_A^j is determined by the energy barrier (peak) seen by the anions when the channel is in its cationic state j.

Current Voltage Relationship

The total current voltage relationship is obtained by summing Eqs. (25*a*), (25*b*) and (27) which gives, after rearrangement and specializing to univalent ions

$$I = e N_s \sqrt{(P_x C'_x + P_y C'_y + P_A C''_A)(P_y C''_y + P_x C''_x + P_A C'_A)}\, 2\sinh \frac{F(U-U_0)}{2RT} \quad (29)$$

where the zero current membrane potential is given by:

$$U_0 = \frac{RT}{F} \ln \frac{P_x C'_x + P_y C'_y + P_A C''_A}{P_x C''_x + P_y C''_y + P_A C'_A} \quad (30)$$

an equation seen to be identical in form to that of the classical Goldman-Hodgkin-Katz equation. The value for N_s is obtained from Eq. (19).

Eqs. (25)–(30) together with Eq. (19) contain the complete description of the transport equations for this system. At this general level there are too many coefficients to be practical and in the following sections the number of parameters will be reduced to a level which approximates to the experimental data measurable for the gramicidin A channel. This procedure will also bring out some of the features characteristic of the model and, in general, of channels containing modulating sites. Anion permeability will be neglected although some effects expected from the entry of anions into the channel will be discussed at the end of the paper.

Factorization of Permeability Expressions and the Physical Meaning of the Coefficients

The cation permeabilities for a binary mixture are seen from Eq. (26) to depend on the concentrations of both cations. This concentration dependence is the result of loading the outer sites, which is apparent from the coefficients of the concentration-dependent terms. A clearer understanding of the physical significance of these coefficients is gained by factorizing the binding constants in a manner shown in Eq. (18). Thus, rewriting Eq. (26*a*),

$$\begin{aligned} P_x = {} & v_{x_i} \cdot k_{x_i} + v_{x_i}^{x_o} \cdot k_{x_i}^{x_o} \cdot k_{x_o} \cdot (C'_x + C''_x) + v_{x_i}^{y_o} \cdot k_{x_i}^{y_o} \cdot k_{y_o} \cdot (C'_y + C'_y) \\ & + v_{x_i}^{x_o x_o} \cdot k_{x_i}^{x_o x_o} \cdot k_{x_o x_o} C'_x C''_x + v_{x_i}^{y_o y_o} \cdot k_{x_i}^{y_o y_o} \cdot k_{y_o y_o} \cdot C'_y C''_y \\ & + v_{x_i}^{y_o x_o} \cdot k_{x_i}^{y_o x_o} \cdot k_{x_o y_o} \cdot (C'_x C''_y + C''_x C'_y). \end{aligned} \quad (31)$$

Because of the unambiguous meaning of the super- and subscripts in this case (note, for instance, that $v_{x_i:}^{:x_o} \cdot k_{x_i:}^{:x_o} = v_{x_i:}^{x_o:} \cdot k_{x_i:}^{x_o:}$ as proved above), the colon sign has been dropped.

It is clear from Eq. (31) that each term contains a product between a binding constant for the inner site, corresponding to a particular state, and a rate constant for jumping across the barrier in the same particular state. Such a product defines a peak energy of the barrier for this state, which is an immediate result of the Eyring rate theory (Woodbury, 1971) and has also been discussed in relation to biological channels by Hille (1975*a*) and by others (Bezanilla & Armstrong, 1972). It is intuitively clear that, since a binding constant defines an energy well and a rate constant defines a barrier height, the product should define the peak energy, in relation to the aqueous phase, which an ion has to surmount in order to pass through the channel.

In summary, therefore, the ionic permeabilities define a set of energy peaks corresponding to the set of cationic states, once the binding constants to the outer sites are known.

An important reduction in the number of coefficients is obtained by assuming the outer sites to be noninteracting with each other. This means, for instance, that $k_{x_o}^{x_o} = k_{x_o}$ and hence $k_{x_o x_o} = k_{x_o}^{x_o} \cdot k_{x_o} = k_{x_o}^2$, etc. It also means that the shift in energy peak on loading the outer sites is additive, i.e.,

$$\frac{v_{x_i}^{x_o x_o} \cdot k_{x_i}^{x_o x_o}}{v_{x_i} \cdot k_{x_i}} = h_{x_i}^{x_o x_o} = e^{\frac{\Delta G_{x_i}^{x_o x_o}}{RT}} = e^{2\frac{\Delta G_{x_i}^{x_o}}{RT}} = h_{x_i}^{x_o} \cdot h_{x_i}^{x_o} \quad \text{etc.}$$

The quantity h defines the energy peak shift which takes place on loading the external sites. Introducing these conditions in Eq. (31) and factorizing yields

$$P_x = \alpha_x (1 + \beta_x C_x' + \beta_y C_y')(1 + \beta_x C_x'' + \beta_y C_y''), \tag{32a}$$

where, taking into account a similar expression for P_y

$$P_y = \alpha_y (1 + \gamma_x C_x' + \gamma_y C_y')(1 + \gamma_x C_x'' + \gamma_y C_y''), \tag{32b}$$

the coefficients are given by

$$\begin{aligned}
&\alpha_x = v_{x_i} \cdot k_{x_i} && \alpha_y = v_{y_i} \cdot k_{y_i} \\
&\beta_x = h_{x_i}^{x_o} \cdot k_{x_o} = \left[\frac{v_{x_i}^{x_o x_o} \cdot k_{x_i}^{x_o x_o}}{v_{x_i} \cdot k_{x_i}}\right]^{\frac{1}{2}} k_{x_o} && \gamma_x = h_{y_i}^{x_o} \cdot k_{x_o} = \left[\frac{v_{y_i}^{x_o x_o} \cdot k_{y_i}^{x_o x_o}}{v_{y_i} \cdot k_{y_i}}\right]^{\frac{1}{2}} k_{x_o} \\
&\beta_y = h_{x_i}^{y_o} \cdot k_{y_o} = \left[\frac{v_{x_i}^{y_o y_o} \cdot k_{x_i}^{y_o y_o}}{v_{x_i} \cdot k_{x_i}}\right]^{\frac{1}{2}} k_{y_o} && \gamma_y = h_{y_i}^{y_o} \cdot k_{y_o} = \left[\frac{v_{y_i}^{y_o y_o} \cdot k_{y_i}^{y_o y_o}}{v_{y_i} \cdot k_{y_i}}\right]^{\frac{1}{2}} k_{y_o}.
\end{aligned} \tag{33}$$

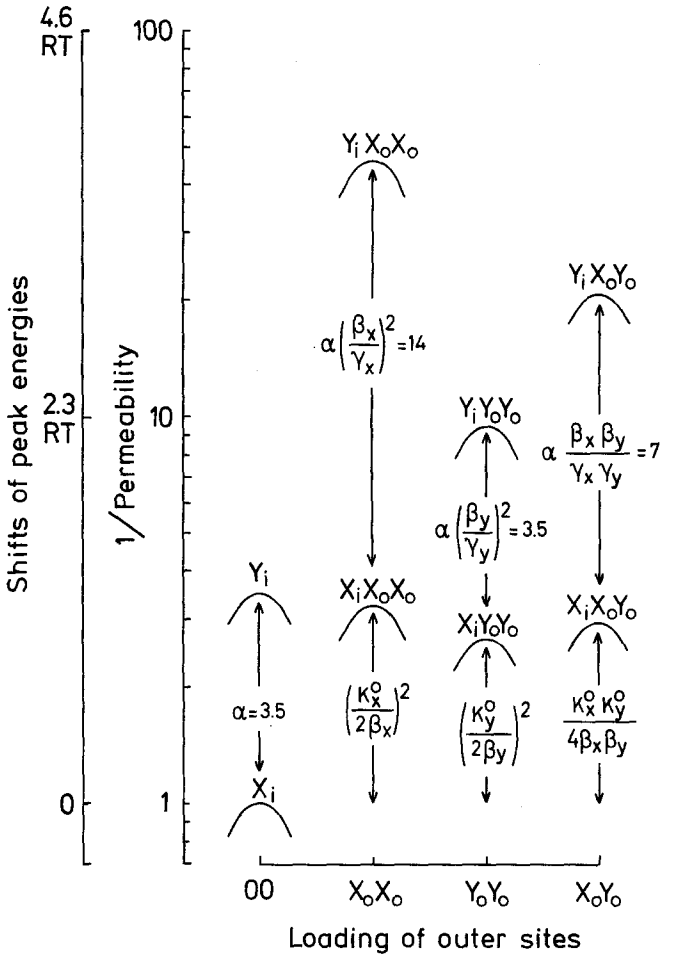

Fig. 4. Diagram showing energy peak shifts (relative to the peak which the ion X encounters in an empty channel) under various indicated conditions of loading. The experimental parameters from which the peak shifts can be calculated are indicated in the figure and the actual values have been taken from Table 1. The constants appearing in the figure are experimentally accessible parameters, defined later in the text

By introducing the condition of noninteracting outer sites, Eq. (1) has now been rigorously proven and the coefficients have been expressed in terms of energy peak shifts and binding constants to the outer sites [Eq. (33)].

The shifts in energy peaks corresponding to the six parameters appearing in Eq. (32) can be illustrated graphically as shown in Fig. 4 for the system thallium (X) – potassium (Y). This binary cation system has been characterized experimentally with respect to permeability ratios (Eisenman

et al., 1976*a*) and single channel conductances (Neher, Eisenman & Sandblom, 1976)[3] where the 6 parameters above have been extracted from experimental data (*also see* Eisenman *et al.*, 1976*b*) (*see* Table 1). The permeability coefficients of Eq. (33) are plotted in Fig. 4 as a function of the loading state of the outer sites, as indicated on the abscissa. Note that the right side peaks are the geometric means of the two other multiple state peaks.

The energy peak differences between the two ions X and Y for each loading state of the outer sites are indicated by arrows in Fig. 4. The magnitude of these arrows are seen, in comparing Eqs. (1) and (33), to be directly obtainable from permeability ratio measurements. The magnitudes of the 4 arrows correspond to 4 different limits of the permeability ratio given by Eq. (32).

$$\frac{P_x}{P_y}=\frac{\alpha_x}{\alpha_y}=\alpha \qquad \begin{matrix} C_x\to 0 \\ C_y\to 0, \end{matrix} \tag{34a}$$

$$\frac{P_x}{P_y}=\frac{\alpha_x}{\alpha_y}\frac{\beta_x^2}{\gamma_x^2} \qquad \begin{matrix} C_x\to \infty \\ C_y\to 0, \end{matrix} \tag{34b}$$

$$\frac{P_x}{P_y}=\frac{\alpha_x}{\alpha_y}\frac{\beta_y^2}{\gamma_y^2} \qquad \begin{matrix} C_x\to 0 \\ C_y\to \infty, \quad \text{and} \end{matrix} \tag{34c}$$

$$\frac{P_x}{P_y}=\frac{\alpha_x\beta_x\beta_y}{\alpha_y\gamma_x\gamma_y} \qquad \begin{matrix} C_x\to \infty \\ C_y\to \infty \quad \text{(biionic)}. \end{matrix} \tag{34d}$$

In Eq. (34*a–c*) the concentrations approach the indicated limits on both sides of the membrane, whereas Eq. (34*d*) applies to the biionic case where the two ions are present on opposite sides.

A condition for having concentration-dependent permeability ratios can now be formulated from Eq. (34), namely, that at least one of the limits are different from the others, i.e., the energy peak shifts are not all equal. This will be referred to as unequal energy peak shifts. Considering that the derivation of Eq. (1) required only the presence of multiple occupancy, the following statement summarizes the permeability properties of a channel: *A multiple occupancy produces concentration-dependent permeabilities, whereas concentration-dependent ratios also require unequal energy peak shifts.*

3 Neher, E., Eisenman, G., Sandblom, J. 1976. Ionic selectivity, binding and block in gramicidin A channels: III. Saturating behavior of single channel conductances and evidence for the existence of two binding sites for monovalent cations on each side of the channel *(in preparation)*.

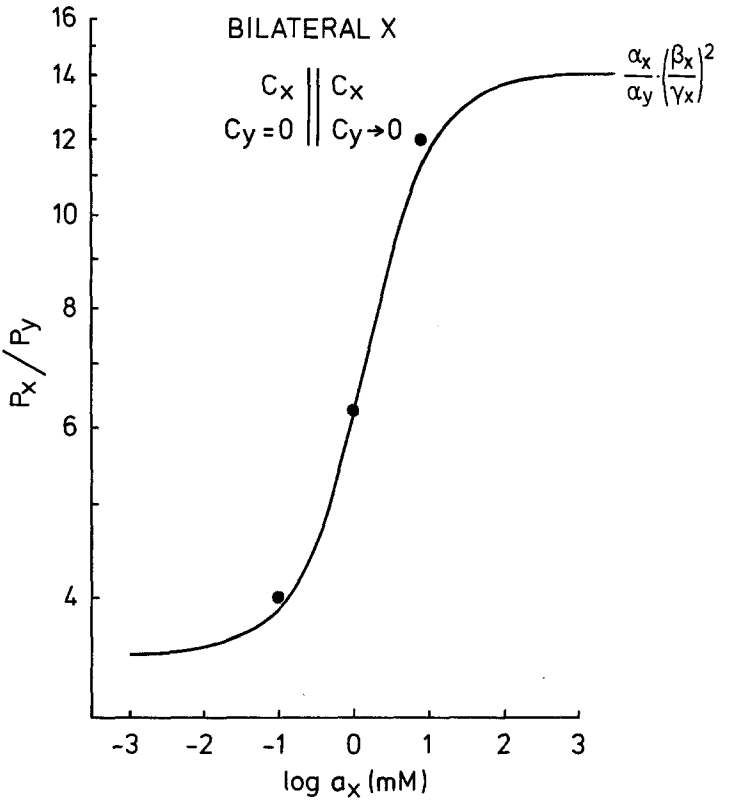

Fig. 5. Theoretical curve for the permeability ratio P_x/P_y calculated from Eq. (32) when the ion X is present symmetrically on both sides of the membrane. The potential is measured when C_y is varied on one side of the membrane which approximates the theoretical condition as C_y is decreased to zero. The theoretical curve is calculated from the parameters of Table 1 and the points are experimentally measured for the system thallium (X)−potassium (Y) in a multichannel system (*GMO*-hexadecane). The permeability ratios have been evaluated from potential data, using the *GHK*-equation [Eisenman *et al.*, 1976 *(in preparation)*]

This is seen more clearly by dividing Eq. (32) to get the permeability ratio

$$\frac{P_x}{P_y}=\frac{\alpha_x}{\alpha_y}\frac{(1+\beta_x C'_x+\beta_y C'_y)(1+\beta_x C''_x+\beta_y C''_y)}{(1+\gamma_x C'_x+\gamma_y C'_y)(1+\gamma_x C''_x+\gamma_y C''_y)}. \tag{32c}$$

The formal requirement for a concentration dependence of this expression is that the coefficients of the terms in $X(\beta_x;\gamma_x)$ and/or the coefficients of the terms in $Y(\beta_y;\gamma_y)$ must not be identical. Since these coefficients give the effects of loading X and Y, respectively, on the permeabilities of X and Y, and have been given explicit energetic meanings in Fig. 4, the requirement of unequal peak shifts to produce concentration dependent permeability ratios is clearly seen.

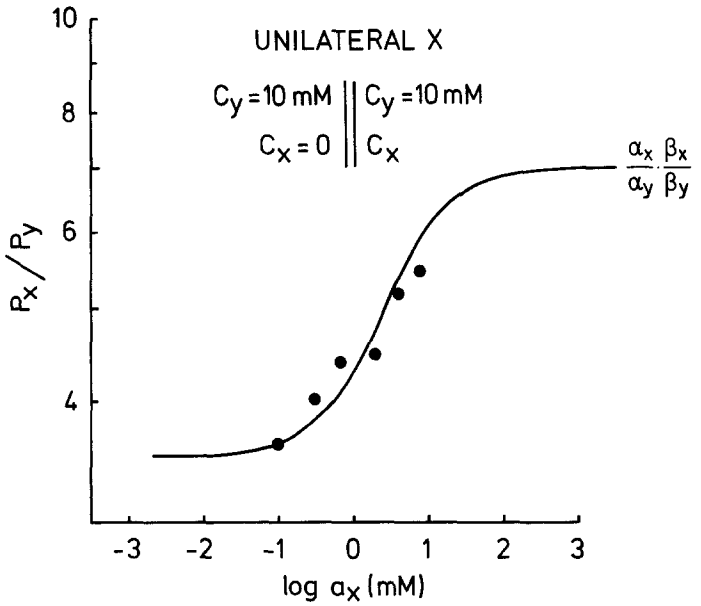

Fig. 6. Theoretical curve for the permeability ratio P_x/P_y calculated from Eq. (32) with values from Table 1 when the ion Y is present in equal amounts (10 mM) on both sides of the membrane and the ion X is varied on one side only. The points are experimentally obtained for the Tl^+-K^+ system [Eisenman *et al.*, 1976*b*]

The general pattern of the permeability ratios, including the limits are shown in Figs. 5, 6 and 7. The curves are drawn according to Eq. (32*c*) (using activities instead of concentrations) and the values for the coefficients are taken from experimental data on the thallium (X)–potassium (Y) system (Eisenman *et al.*, 1976*b*) (Table 1).

The concentration dependence of the permeability ratios is the result of ion interactions in the channel which lead either to an increase (enhancement) or to a decrease (block) in the permeability ratios on loading the outer sites. If, for instance, $\beta_x/\gamma_x > 1$ the effect of X on the channel is to enhance the permeability of X relative to Y on loading the external sites, whereas if $\beta_x/\gamma_x < 1$ the effect is opposite. These effects are illustrated most clearly in Fig. 8 in which the permeability ratio P_x/P_y is plotted against $1/C_x$ at the high concentration end, where X is varied only on one side, while the other variables are kept constant. In the same figure are the values obtained from a paper by Cahalan and Begenisich (1976) where they have plotted P_K/P_{Na}, against $1/\alpha_K$ for the sodium channel in squid axons.

In view of the similar behavior of sodium channels and gramicidin A channels and the ability of the model to describe the general pattern of

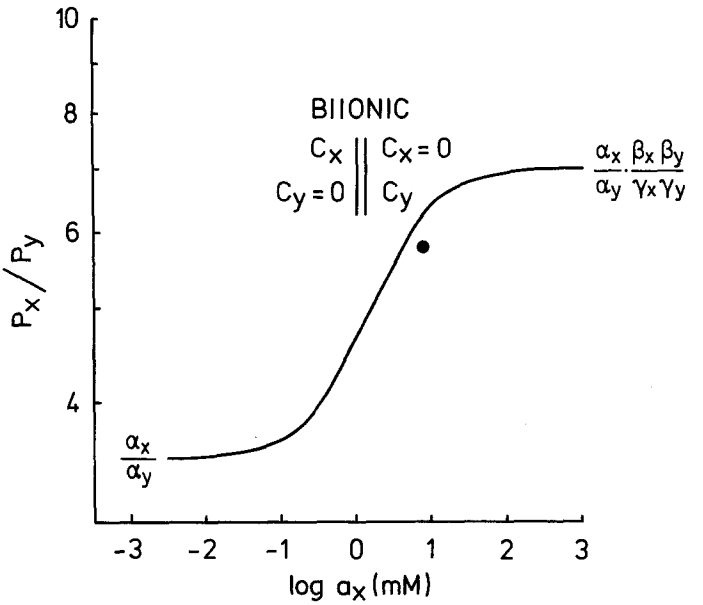

Fig. 7. Theoretical curve calculated from Eq. (32) with values taken from Table 1 in the biionic case. The point is experimentally obtained for the Tl^+-K^+ case (Eisenman *et al.*, *in preparation*)

concentration-dependent permeability ratios, it seems reasonable to conclude that the presence of several simultaneously occupiable binding sites and correspondingly different conductance states is a general property of ionic channels.

Conductance at Zero Current in Symmetrical Solutions

The permeability ratios were shown in the previous section to yield some very important pieces of information about the properties of the channel and the nature of ion interactions. However, it is not possible from Eq. (32) to separate energy peak shifts from binding constants and this missing piece of information is most conveniently obtained from measurements of the conductance in symmetrical solutions.

In the following, the anion permeability will be neglected and therefore, according to Eq. (29), the conductance G $\left(\text{normalized with respect to } \frac{eF}{RT}\right)$ at zero current reduces to

$$G = N_s(P_x C_x + P_y C_y). \tag{35}$$

P_x and P_y are obtained from Eq. (26) and N_s is obtained from Eq. (19).

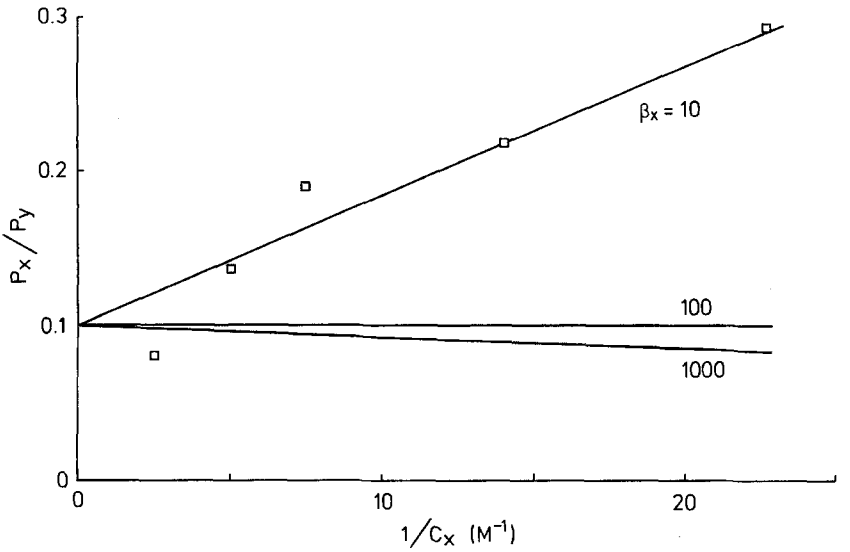

Fig. 8. The permeability of X relative to Y is plotted against $1/C'_x$ according to Eq. (32) under a particular set of conditions, namely that C''_x, C''_y are held constant and $\beta_y C'_y$, $\gamma_y C'_y$ assumed to be negligibly small. Eq. (32) can then be written as[4] If the sites are noninter

$$\frac{P_x}{P_y} = a\left(1 + \frac{\left(\frac{\gamma_x}{\beta_x} - 1\right)}{1 + \gamma_x C_x}\right).$$

a is set equal to 0, 1 and $\gamma_x = 0.1/\text{M}$. β_x is assigned 3 different values as indicated in the figure. The squares are the values of P_K/P_{Na} for squid axons (Cahalan & Begenisich, 1976) where the potassium concentration (corresponding to C'_x) is varied on the inside

(a) Single Cation Salt

The conductance expression Eq. (35) is written explicitly for a single salt by setting C'_y, C''_y equal to zero and $C'_x = C''_x$. Inserting these conditions in the permeability expression (32*a*) and the expression for N_s (Eq. 19), the conductance Eq. (35) assumes the following form:

$$G = \frac{P_1 C_x + 2P_2 C_x^2 + P_3 C_x^3}{1 + 2K_1 C_x + K_2 C_x^2 + 2K_3 C_x^3 + K_4 C_x^4}, \tag{36}$$

where

$$P_1 = v_{x_i} \cdot k_{x_i}, \tag{37a}$$

$$P_2 = v_{x_i}^{x_o} \cdot k_{x_i}^{x_o} \cdot k_{x_o}, \tag{37b}$$

$$P_3 = v_{x_i}^{x_o x_o} \cdot k_{x_i}^{x_o x_o} \cdot k_{x_o x_o}; \tag{37c}$$

and

$$K_1 = k_{x_o} + k_{x_i}, \tag{38a}$$

$$K_2 = k_{x_o x_o} + k_{x_i x_i} + 2k_{x_o x_i}, \tag{38b}$$

$$K_3 = k_{x_o x_i x_o} + k_{x_o x_i x_i}, \tag{38c}$$

$$K_4 = k_{x_o x_i x_i x_o}. \tag{38d}$$

The sum $(k_{x_o:x_i} + k_{x_o x_i:})$ has been abbreviated in the symbol $k_{x_o x_i}$ appearing in Eq. (38*b*). All other constants are unambiguously defined.

In order to extract the parameters appearing in Eqs. (37) and (38) from experimental data it is useful to rearrange Eq. (36) to yield an Eadie-Hofstee plot, frequently used to characterize a system showing saturation kinetics. The Eadie-Hofstee representation is given by

$$G = G_x - \frac{G}{C_x}\frac{1}{K} \tag{39}$$

where K is a binding constant and G_x the maximum (saturation) conductance of ion X.

Rearranging Eq. (36) in a form which resembles Eq. (39) yields an equation with two concentration-dependent coefficients,[4]

$$G = \frac{P_1 + 2P_2 C_x + P_3 C_x^2}{2K_1 + 2K_3 C_x^2} - \frac{G}{C_x} \cdot \frac{1 + K_2 C_x^2 + K_4 C_x^4}{2K_1 + 2K_3 C_x^2}. \tag{40}$$

Depending on the concentration range, the limiting behavior of this equation can be divided in three parts. For low ion concentrations

$$G = G_x^o - \frac{G}{C_x} \cdot \frac{1}{K_x^o} \tag{41}$$

where

$$G_x^o = \frac{P_1}{2K_1} = \frac{1}{2} v_{x_i} \cdot \frac{k_{x_i}}{k_{x_o} + k_{x_i}}, \tag{42a}$$

$$K_x^o = 2K_1 = 2(k_{x_o} + k_{x_i}). \tag{42b}$$

For high concentrations (assuming $K_4 \ll K_2^2$) Eq. (40) has the same limiting behavior

$$G = G_x^h - \frac{G}{C_x} \cdot \frac{1}{K_x^h} \tag{43}$$

with

$$G_x^h = \frac{P_3}{2K_3} = \frac{1}{2} \frac{v_{x_i}^{x_o x_o} \cdot k_{x_i}^{x_o x_o} \cdot k_{x_o x_o}}{k_{x_o x_i x_o} + k_{x_o x_i x_i}}, \tag{44a}$$

$$K_x^h = \frac{2K_3}{K_2} = 2 \frac{k_{x_o x_i x_o} + k_{x_o x_i x_i}}{k_{x_o x_o} + k_{x_i x_i} + 2k_{x_o x_i}}. \tag{44b}$$

[4] If the sites are noninteracting, then $P_2^2 = P_1 P_3$ (Eq. (37)) and if $k_{x_o} \gg k_{x_i}$ then $k_2 = k_1^2$ (Eq. (38)), which reduces the number of independent parameters.

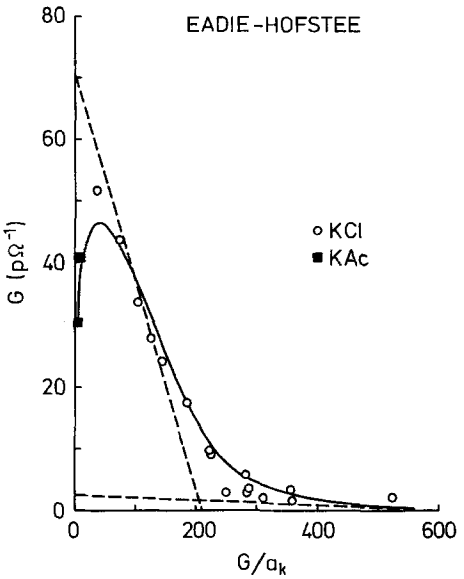

Fig. 9. Eadie-Hofstee plot constructed according to Eq. (36) with values taken from Table 1. The asymptotes, shown as dotted lines, are drawn from Eqs. (41) and (43), respectively. The experimentally observed conductances obtained from single channel conductances (*GMO*-hexadecance) for KCl (circles) and KAc (filled squares) (Neher *et al., in preparation*) are included in the figure for comparison

Finally, as the concentration C_x increases towards infinity, the conductance approaches zero with the following limiting behavior:

$$\log G = \log G_x^h - \log C K_x^\infty \tag{45}$$

where

$$K_x^\infty = \frac{K_4}{2K_3} = \frac{1}{2} \frac{k_{x_o x_i x_i x_o}}{k_{x_o x_i x_o} + k_{x_o x_i x_i}}. \tag{46}$$

The parameters in Eqs. (41)-(46), (K_x^o, K_x^h, K_x^∞, G_x^o, G_x^h) are all experimentally measurable. K_x^o and K_x^h are binding constants and G_x^o and G_x^h are maximum limiting conductances for the low (superscript "*o*") and high (superscript "*h*") concentration asymptotes in Eadie-Hofstee plots. An example is shown in Fig. 9 for the potassium ion. Fig. 9 compares the experimentally observed conductances (data points) with the theoretical curve (for Eq. 36). It shows clearly not only the regions of concentration dependence corresponding to Eqs. (41) and (43) but also shows the decrease in conductance at the very highest concentrations expected from Eq. (36).

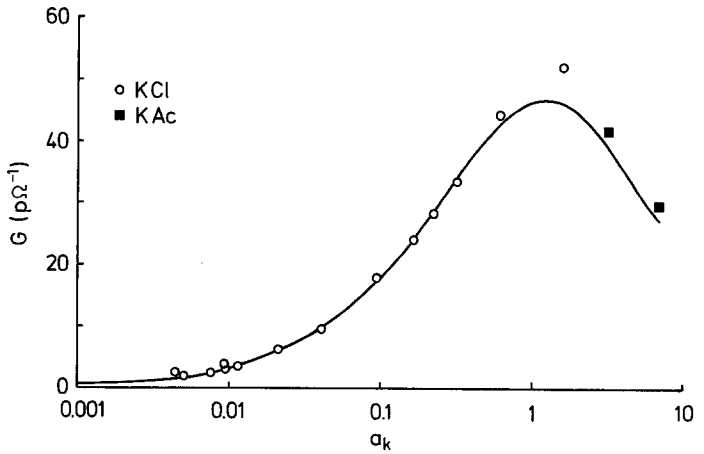

Fig. 10. A direct representation of the conductance as a function of concentration using the same theoretical and experimental values as shown in Fig. 9

The same values and data points appear in Fig. 10, which shows a plot of conductance *vs.* concentration. The ability of Eq. (36) to fit the data over such a wide range of concentrations lends additional support to the idea that at least four ions can occupy the channel at a time.

Comparison with Potential Data

Certain of the parameters assessed from conductances can be related to the parameters appearing in the permeability expressions. Comparing Eqs. (42) and (33), the following relationships are deduced:

$$G_x^o \cdot K_x^o = v_{x_i} \cdot k_{x_i} = \alpha_x; \tag{47a}$$

$$G_y^o \cdot K_y^o = v_{y_i} \cdot k_{y_i} = \alpha_y. \tag{47b}$$

The product of the limiting conductance and binding constant at low concentrations is therefore a measure of the energy peak of the unloaded channel, and the ratio between these products therefore expresses the energy peak shift, a quantity which is also obtained from potential measurements at low concentrations [Eq. (34)].

Any further comparison between conductances and potential data is impossible without making some further assumption which will reduce the many binding constants, unseparable by electrical measurements, which appear in Eqs. (42), (44) and (46). A reasonable assumption, which proves to be very useful, is to consider the binding constants for the inner

sites to be small in comparison with the binding constants for the outer sites (i.e., $k_{x_o} \gg k_{x_i}$, $k_{x_o x_i : x_o} \gg k_{x_o x_i : x_i}$, etc.). Eqs. (42), (44) and (46) then reduce to

$$G_x^o = \frac{v_{x_i} \cdot k_{x_i}}{2 k_{x_o}}; \tag{48a}$$

$$K_x^o = 2 k_{x_o}; \tag{48b}$$

$$G_x^h = \tfrac{1}{2} v_{x_i}^{x_o x_o}; \tag{48c}$$

$$K_x^h = 2 k_{x_i}^{x_o x_o}; \tag{48d}$$

$$K_x^\infty = \tfrac{1}{2} k_{x_i}^{x_o x_o x_i}. \tag{48e}$$

Moreover, it follows that

$$G_x^h K_x^h = v_{x_i}^{x_o x_o} \cdot k_{x_i}^{x_o x_o} = \alpha_x \cdot h_x^{x_o x_o} = 4 \alpha_x \beta_x^2 / K_x^{o^2}, \tag{49a}$$

and similarly for Y,

$$G_y^h K_y^h = 4 \alpha_y \gamma_y^2 / K_y^{o^2}. \tag{49b}$$

Experimental data on the thallium-potassium system have satisfactory verified Eqs. (47) and (49) (*see* Eisenman *et al.*, 1976*b* and Table 1). This is a good test of the model, but it does not constitute a justification for the assumption that $k_{x_o} \gg k_{x_i}$. The experimental data can be used to arrive at Eq. (49) in a different way, namely, by assuming the inner sites as well as the outer sites to be noninteracting; in other words, assuming completely noninteracting channel halves. Eqs. (44) then transform to

$$\alpha_x \beta_x^2 = v_{x_i}^{x_o x_o} \cdot k_{x_i}^{x_o x_o} \cdot k_{x_o}^2 = G_x^h K_x^h \frac{1}{4} K_x^{o^2} \left(1 + \frac{K_x^h}{K_x^o - 2 K_x^h}\right), \tag{50}$$

which, since $K_x^o \gg K_x^h$, reduces to Eq. (49*a*). The same applies to Eq. (49*b*).

The advantage of assuming that $k_{x_o} \gg k_{x_i}$, however, is that the peak shifts can be evaluated from Eq. (33) and represented in a diagram such as that given in Fig. 4. A diagram of this sort provides a key to the understanding of the molecular mechanisms which govern the transport properties and ion interactions taking place in the channel.

(b) Two Cation Mixtures

Having defined a set of measurable channel parameters from conductances in single salt solutions, it is now of interest to examine the extent to which the model predicts the minimum in conductance and the blocking tendency reported by Neher (1975) for binary mixtures.

If this analysis is carried out in the region of concentrations where the fourth order terms appearing in Eq. (19) can be neglected, Eq. (19) will contain only two additional experimentally undetermined constants, corresponding to the mixed terms, namely, K^h_{xxy} and K^h_{yyx} defined through Eq. (51),

$$\tfrac{1}{2}(k_{x_o})^2 K^h_{xxy} = k_{y_o:x_i x_o} + k_{y_i:x_i x_o} + k_{x_o:x_i y_o} + k_{x_o:y_i x_o} + k_{x_i:y_i x_o} + k_{x_i:x_o y_o}. \quad (51a)$$

$$\tfrac{1}{2}(k_{y_o})^2 K^h_{xyy} = k_{x_o:y_i y_o} + k_{x_i:x_i y_o} + k_{y_o:y_i x_o} + k_{y_o:x_i y_o} + k_{y_i:y_i x_o} + k_{y_i:x_i y_o}. \quad (51b)$$

The final expression for G (Eq. 35) can now be written, neglecting fourth order terms, and putting $k_{x_o} \gg k_{x_i}$, $k_{y_o} \gg k_{y_i}$,

$$G = \frac{P_x C_x}{\left(1 + \frac{K^o_x}{2} C_x + \frac{K^o_y}{2} C_y\right)^2 + K^h_x C_x (\tfrac{1}{2} K^o_x C_x)^2 + K^h_y C_y (\tfrac{1}{2} K^o_y C_y)^2 + P_y C_y + (\tfrac{1}{2} K^o_x C_x)^2 K^h_{xxy} C_y + (\tfrac{1}{2} K^o_y C_y)^2 K^h_{yyx} C_x}. \quad (52)$$

Fig. 11 shows the conductance as a function of mole fraction in Tl-K ($X - Y$) mixtures at the indicated concentration levels. The curves are calculated from Eq. (52) with values for the constants taken from Table 1. K^h_{TlTlK} is set equal to zero and K^h_{KKTl} is assigned two different values (0 and 1000 per M, corresponding to the solid and dotted curves). A minimum in conductance is clearly seen at low concentrations and at higher concentrations the conductance shows a maximum (for $K^h_{\mathrm{KKTl}} = 0$). This complex pattern of conductance behavior is the combined result of the concentration-dependent permeabilities and the concentration-dependent N_s appearing in Eq. (52).

(c) Block of Channel Conductance in Ionic Mixtures

Eq. (52) also predicts a blocking effect of Tl on the Na-conductance reported by Neher (1975) and illustrated in Fig. 12. In this figure the conductance is represented as a Lineweaver-Burk plot, i.e., $1/G$ against $1/C$, and the upper curve shows the shift in binding constant for sodium on adding a small amount (2 mM) of thallium.

In order to show how this effect can be explained in terms of Eq. (52) only the binding behavior at high concentrations needs to be considered. Inverting Eq. (52) to obtain the Lineweaver-Burk representation of ion X,

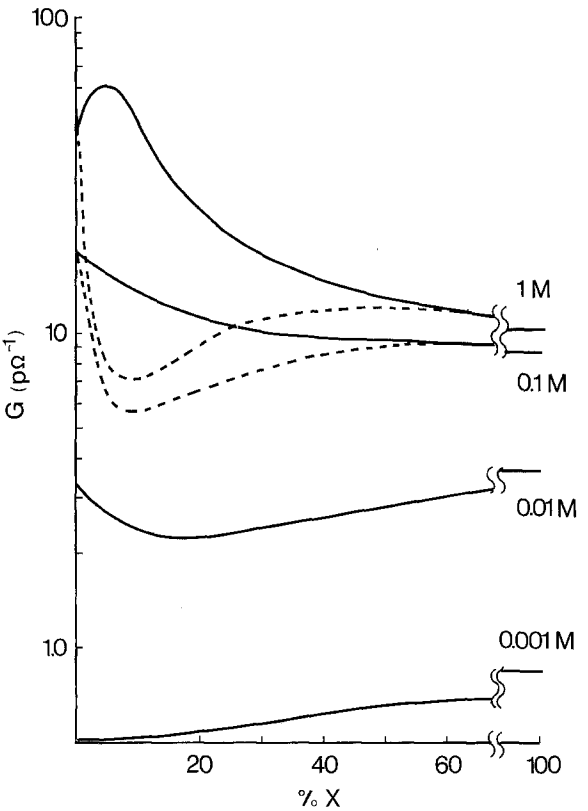

Fig. 11. The conductance in mixtures of Tl (X) and K (Y) at equal total concentrations (as indicated) and identical solutions on both sides of the membrane. The abscissa gives the percentage of X in solution. The solid curves are calculated from Eq. (52) with values obtained from Table 1 and K^h_{yyx}, $K^h_{xxy}=0$. If, instead, K^h_{yyx} is set equal to 5000/M in Eq. (52), keeping the other parameters the same, a different set of curves (dotted lines) are obtained at the highest concentrations

and taking the limit at high concentrations C_x, the following terms remain:

$$\frac{1}{G_x}=\frac{K^h_x(\frac{1}{2}K^o_x)^2}{\alpha_x\beta^2_x}+\frac{1}{C_x}\frac{(\frac{1}{2}K^o_x)^2(1+K^h_{xxy}C_y)}{\alpha_x\beta^2_x}. \tag{53}$$

The first term on the right side is the inverse saturation conductance of X. This is seen to be unaffected by the addition of Y and which is consistent with experimental observations (Fig. 12).

The last term in Eq. (53) defines the product of an apparent binding constant and the limiting conductance. Dividing the two terms on the

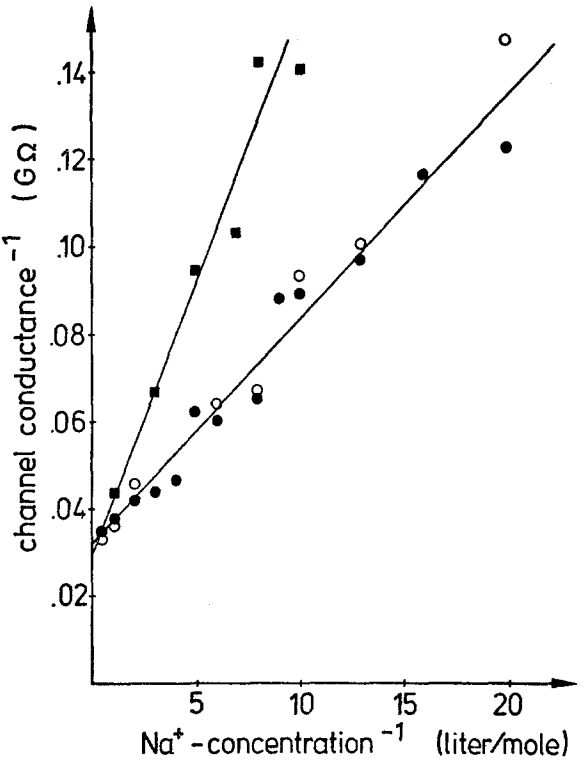

Fig. 12. The reciprocal conductance of Gramicidin A single channels in symmetrical solutions of TlAc and NaAc plotted against the reciprocal of sodium concentration (Lineweaver-Burk representation). The salt is pure NaAc for circles (open symbols refer to conductance at 100 mV applied potential and filled symbols are zero potential values). The squares are values obtained when the salt is NaAc in the presence of a constant amount of 2 mM TlAc. Replotted after Neher (1975)

right hand side of Eq. (53) therefore yields the apparent binding constant

$$(K_x^h)_{\text{app}} = \frac{K_x^h}{1 + K_{xxy}^h C_y}. \tag{54a}$$

Similarly for the ion y,

$$(K_y^h)_{\text{app}} = \frac{K_y^h}{1 + K_{yyx}^h C_x}. \tag{54b}$$

Eq. (54) clearly demonstrates the mutual blocking effect of two ions in terms of a decrease in the apparent binding constant for one ion following the addition to the external solutions of the other ion. They also contain the information necessary to extract the values of K_{xxy}^h and K_{yyx}^h from conductances in ionic mixtures.

It should be noted that Eq. (54) predicts a decrease in apparent binding constants, i.e., an inhibitory effect on the passage of an ion. However, this inhibitory effect on the conductance can be coupled to an enhancement seen in the permeability ratio (*see* Fig. 8). This seemingly contradictory effect is due to the fact that the permeability ratio contains the blocking effect which an ion, say Y, exerts on itself, and which can be larger than the blocking effect on the other ion X. This leads to an enhancement in the permeability of X relative to Y and at the same time an inhibition of the conductance G_x in the presence of Y. A discrepancy between conductance ratios and permeability ratios has been reported by Myers and Haydon (1972) and is accounted for by the present theory (Eisenman *et al.*, 1976*b*) through Eqs. (32) and (36).

Additional Properties when Anion Permeability is not Negligible

Although, in agreement with the conclusion of Myers and Haydon (1972) that the gramicidin channel is impermeant to anions relative to the usual monovalent cations, anion permeability will also be shown to be negligible in the presence of Tl^+ in the following two experimental papers [Eisenman *et al.*, 1976 *(in preparation)*; Neher *et al. (in preparation)*], we have encountered experimental situations using acetate and nitrate where anion permeability can become significant (Eisenman *et al.*, 1976*a*, 1976*b*). To consider extensively here the theoretically expected effects of a finite anion permeability would go beyond the purpose of this paper to provide a theory adequate to deal with the data when anion permeation is negligible; but it is appropriate to point out briefly how a finite permeability to anions would be expected to influence the experimental observations.

If, by setting $P_A = 0$ in Eq. (30), an apparent permeability ratio (P_x/P_y) is calculated from potential measurements, this estimate will deviate from the true permeability ratio if the anion permeability is significant. Depending on the external solution conditions the apparent permeability ratio will then either be an overestimate or an underestimate of the true permeability ratio. One way to estimate this error is to perform "delta" experiments of the type described in Table V and Fig. 18 of Eisenman *et al.* (1976*b*) in which the apparent permeability ratios are measured for the same symmetrical initial conditions by making a small gradient in the concentration of X (or Y) by adding a small "delta" increment X (or Y), to one side. Such an experiment yields apparent permeability ratios which

are different for the two increments only if there is anion permeation through the channel [Eisenman *et al.* 1976 *(in preparation)*].

A finite anion permeability can also affect the observed conductance for single channels. However, a difference in conductance (or true permeability ratio) observed with different anions does not *per se* unambiguously demand the existence of a significant anion permeability since a possible anionic modulation of the cation conductance (e.g., by binding, but without necessarily permeating) must also be considered. Such an ambiguity is not present in the comparison of apparent permeability ratios measured by membrane potential in gradients of X *vs.* gradients of Y, i.e., "delta" experiments. It is therefore possible to sort out the different anion effects as will be described in later papers of this series.

Discussion

Previous theoretical treatments have considered either 1-ion saturable channels (Läuger, 1973) or, at most, occupancy of 2 sites by 2 ions (Hladky, 1972, 1974). Our theoretical treatment has shown that many of the features characteristic of ion interactions in a channel such as concentration-dependent ion selectivities, saturation phenomena and block demand extension to a 4-site model of the channel, all 4 sites being capable of simultaneous occupancy by cations. The general treatment of this model was shown to produce 92 parameters for a two-cation mixture (80 binding constants and 12 rate constants) which is totally impractical from an experimental point of view. However, by assuming the outer sites to be mutually noninteracting and that the outer sites bind much more strongly than the inner sites, it was shown that the number of independent parameters needed to characterize the transport properties of the channel, excluding the 4-occupancy states, was reduced to 12 (6 binding constants and 6 rate constants). The measurable parameters are summarized in Table 2 and only 12 of those are needed to characterize the channel.

The addition of 4-occupancy states, which are not associated with the transport of ions since all sites are occupied, introduces additional binding constants which can be evaluated from the limiting behavior of the channel conductances at very high concentrations. If the inner sites do not mutually interact, however, the 4-occupancy parameters can be obtained from the other binding constants appearing in Table 2.

Generalizations

The properties of the 4-site model are not greatly altered if the number of barriers is increased with some additional restrictions. Assuming that

Table 2. Relationships between experimental and theoretical parameters[a]

Measured parameter	Physical parameter	
$\alpha=\frac{\alpha_x}{\alpha_y}$	$\frac{v_{x_i}\cdot k_{x_i}}{v_{y_i}\cdot k_{y_i}}$	
β_x, β_y	$\left(\frac{v_{x_i}^{x_o x_o}\cdot k_{x_i}^{x_o x_o}}{v_{x_i}\cdot k_{x_i}}\right)^{\frac{1}{2}} k_{x_o}$,	$\left(\frac{v_{x_i}^{y_o y_o}\cdot k_{x_i}^{y_o y_o}}{v_{x_i}\cdot k_{x_i}}\right)^{\frac{1}{2}} k_{y_o}$
γ_x, γ_y	$\left(\frac{v_{y_i}^{x_o x_o}\cdot k_{y_i}^{x_o x_o}}{v_{y_i}\cdot k_{y_i}}\right)^{\frac{1}{2}} k_{x_o}$,	$\left(\frac{v_{y_i}^{y_o y_o}\cdot k_{y_i}^{y_o y_o}}{v_{y_i}\cdot k_{y_i}}\right)^{\frac{1}{2}} k_{y_o}$
G_x^o, G_y^o	$\frac{1}{2} v_{x_i}\cdot\frac{k_{x_i}}{k_{x_o}+k_{x_i}}\approx\frac{1}{2} v_{x_i}\cdot\frac{k_{x_i}}{k_{x_o}}$,	$\frac{1}{2} v_{y_i}\cdot\frac{k_{y_i}}{k_{y_o}+k_{y_i}}\approx\frac{1}{2} v_{y_i}\cdot\frac{k_{y_i}}{k_{y_o}}$
G_x^h, G_y^h	$\frac{1}{2}\left(\frac{v_{x_i}^{x_o x_o}\cdot k_{x_i}^{x_o x_o}\cdot k_{x_o}}{k_{x_o x_i x_o}+k_{x_o x_i x_i}}\right)^2\approx\frac{1}{2} v_{x_i}^{x_o x_o}$,	$\frac{1}{2}\left(\frac{v_{y_i}^{y_o y_o}\cdot k_{y_i}^{y_o y_o}\cdot k_{y_o}}{k_{y_o y_i y_o}+k_{y_o y_i y_i}}\right)^{\frac{1}{2}}\approx\frac{1}{2} v_{y_i}^{y_o y_o}$
K_x^o, K_y^o	$2(k_{x_o}+k_{x_i})\approx 2k_{x_o}$,	$2(k_{y_o}+k_{y_i})\approx 2k_{y_o}$
K_x^h, K_y^h	$2\left(\frac{k_{x_o x_i x_o}+k_{x_o x_i x_i}}{k_{x_o x_o}+k_{x_i x_i}+2k_{x_o x_i}}\right)\approx 2k_{x_i}^{x_o x_o}$,	$2\left(\frac{k_{y_o y_i y_o}+k_{y_o y_i y_i}}{k_{y_o y_o}+k_{y_i y_i}+2k_{y_o y_i}}\right)\approx 2k_{y_i}^{y_o y_o}$
K_x^∞, K_y^∞	$\frac{1}{2}\frac{k_{x_o x_i x_i x_o}}{k_{x_o x_i x_o}+k_{x_o x_i x_i}}\approx\frac{1}{2} k_{x_i}^{x_o x_i x_o}$,	$\frac{1}{2}\frac{k_{y_o y_i y_i y_o}}{k_{y_o y_i y_o}+k_{y_o y_i y_i}}\approx\frac{1}{2} k_{y_i}^{y_o y_i y_o}$
K_{xxy}^h, K_{yyx}^h	$\approx 2k_{y_i}^{x_o x_o}+2k_{x_i}^{x_o y_o}\cdot\frac{k_{y_o}}{k_{x_o}}$,	$\approx 2k_{x_i}^{y_o y_o}+2k_{y_i}^{x_o y_o}\cdot\frac{k_{x_o}}{k_{y_o}}$
$\alpha_x=G_x^o\cdot K_x^o$, $\alpha_y=G_y^o\cdot K_y^o$	$v_{x_i}\cdot k_{x_i}$,	$v_{y_i}\cdot k_{y_i}$
$G_x^h\cdot K_x^h, G_y^h\cdot K_y^h$	$\approx v_{x_i}^{x_o x_o}\cdot k_{x_i}^{x_o x_o}$,	$\approx v_{y_i}^{y_o y_o}\cdot k_{y_i}^{y_o y_o}$

[a] The table also contains the forms to which the relationships reduce when $k_{x_o}\gg k_{x_i}$, $k_{y_o}\gg k_{y_i}$, etc.

configurations involving more than one ion are restricted to those in which the outer sites are loaded and only one ion occupies any one of the inner sites, the rate equations for the transport of a univalent cation X through the channel are extended from Eq. (25),

$$\begin{aligned} I_x &= e\vec{P}_x' C_x' N_s e^{\frac{FU}{2nRT}} - e\overleftarrow{P}_x' N_x' e^{-\frac{FU}{2nRT}} \\ I_x &= e\vec{P}_x^n N_x^n e^{\frac{FU}{2nRT}} - e\overleftarrow{P}_x'' C_x'' N_s e^{-\frac{FU}{2nRT}}, \end{aligned} \tag{55}$$

where the permeabilities P_x^i are equal in form to Eq. (1). If the barriers have equal heights or if they otherwise satisfy a set of conditions listed by Läuger (1973), the membrane potential at zero current will satisfy Eq. (30) and therefore remain unaltered.

The form of the conductance expression, Eq. (36), will also remain unaltered by this extension of the model except for the absence of a fourth order term. An important difference, however, concerns the parameters K which will now become voltage-dependent [*compare* Läugers treatment (1973)]. The need for this extension of the model should therefore depend on the outcome of experimental tests.

The fourth order term in the conductance Eq. (36) can also be introduced in the extended model by assuming that the channel can be occupied by 4 ions in one particular configuration only, namely, the outermost inner sites, and this consequently blocks the channel. If more than one configuration of 4 ions is permitted, Eq. (55) must be extended and the transport properties will furthermore exhibit the phenomenon of single filing. This again is accessible to experimental test most easily by measuring the undirectional flux ratios.

The four-site model can be applied to biological channels, notably the sodium channel, in order to characterize the observed concentration dependence of ionic selectivities (Begenisich & Cahalan, 1975; Cahalan & Begenisich, 1976) as well as the phenomena of saturation and block (Hille, 1975*a*; 1975*b*). However, to account for the nonlinearities in the I–V curves an extension to several barriers is required corresponding to the theoretical treatments by, Hille (1975*a*), Heckman *et al.* (1972) and by Läuger (1973).

The model analyzed in this paper seems nevertheless to fit the data accumulated so far on the gramicidin A channel [Eisenman *et al.*, 1976 *(in preparation)*, Neher *et al.*, 1976 *(in preparation)*], and it should, therefore, be of general usefulness in characterizing intra-channel ionic interactions from such experimentally observed phenomena as concentration-dependent ion selectivities, saturation and block in membranes containing ionic channels. The nature of the ionic interactions are as yet unknown and a clear understanding of their physical origin will probably require a set of experiments giving the energy diagram of Fig. 4 for a large variety of cations. It seems reasonable at this stage, however, to conclude that the relatively large differences in peak shifts seen in Fig. 4 are difficult to reconcile with purely electrostatic repulsive forces. Some other mechanism, such as induction effects, is probably responsible for the large shifts in energy peaks produced by the exchange of ions at the outer sites. For example, if loading various external cations alters the "field strength" of the binding sites (and energy barriers) it can be inferred from well-known effects of "field strength" on selectivity (Eisenman, 1961, 1962) that such a "field strength" effect would directly imply a differential shift in the level

of the wells and also implicitly (*cf.* Hille, 1975*a*) imply differential shifts of the peaks in the activation energy profile.

This work was supported by National Science Foundation Grant GB 30835, U.S. Public Health Services Grant NS09931 and Swedish Medical Research Council grant 04138.

References

Andersen, O.S. 1975. Ion-specificity of gramicidin channels. *Int. Biophys. Congress, Copenhagen.* p. 369

Begenisich, T., Cahalan, M. 1975. Internal K^+ alters sodium channel selectivity. *Int. Biophys. Congress, Copenhagen.* p. 133 *(Abstr.)*

Bezanilla, F., Armstrong, C.M. 1972. Negative conductance caused by entry of sodium and cesium ions into the potassium channels of squid axons. *J. Gen. Physiol.* **60**:588

Cahalan, M., Begenisich, T. 1976. Sodium channel selectivity: Dependence on internal permeant ion concentration. *J. Gen. Physiol.* **68**:111

Eisenman, G. 1961. On the elementary atomic origin of equilibrium ionic specificity. *In: Symposium on Membrane Transport and Metabolism.* A. Kleinzeller and A. Kotyk, editors. p. 163. Academic Press, New York

Eisenman, G. 1962. Cation selective glass electrodes and their mode of operation. *Biophys. J.* **2 (2)**:259

Eisenman, G., Krasne, S., Ciani, S. 1974. Further studies on ion selectivity. Proceedings of International Workshop on Ion-Selective Electrodes and on Enzyme Electrodes in Biology and in Medicine, M. Kessler, L. Clark, D. Lübbers, I. Silver and W. Simon, editors. Urban and Schwarzenberg, Münich, Berlin, Vienna *(in press)*

Eisenman, G., Sandblom, J., Neher, E. 1976*a*. Evidence for multiple occupancy of gramicidin A channels by ions. *Biophys. Soc. Annu Meet. Abstr.* p. 81*a*

Eisenman, G., Sandblom, J., Neher, E. 1976*b*. Ionic selectivity, saturation, binding and block in the gramicidin A channel: A preliminary report. *9th Jerusalem Symp. on Metal-Ligand Interactions in Organic and Biochemistry.* B. Pullman and N. Goldblum, editors. D. Reidel, Dordrecht *(in press)*

Eyring, H., Lumry, R., Woodbury, J.W. 1949. Some applications of modern rate theory to physiological systems. *Rec. Chem. Prog.*, **10**:100

Heckman, K. 1972. Passive Permeability of Cell Membranes, Biomembranes, F. Kreuzer and J.F.G. Slegers, editors. Vol. 3, p. 127. Plenum press, New York

Heckman, K., Lindemann, B., Schnakenberg, J.S. 1972. Current-voltage curves of porous membranes in the presence of pore-blocking ions. I. Narrow pores containing no more than one moving ion. *Biophys. J.* **12**:683

Heckman, K., Vollmerhaus, Z. 1970. Zur Theorie der "Single File"-Diffusion. IV. Vergleich von Leerstellendiffusion und "knock-on"-Mechanismus. *Phys. Chem. (NF)* **71**:320

Hille, B. 1975*a*. Ionic selectivity of Na and K channels of nerve membranes. *In:* Membranes – A Series of Advances, Vol. 3, Ch. 4. Dynamic Properties of Lipid Bilayers and Biological Membranes, G. Eisenman, editor. Marcel Dekker, New York

Hille, B. 1975*b*. Ionic selectivity, saturation, and block in sodium channels. *J. Gen. Physiol.* **66**:535

Hladky, S.B. 1972. The Two-Site Lattice Model for the Pore. Ph.D. Dissertation, Cambridge University, England

Hladky, S.B. 1974. Pore or carrier? Gramicidin A as a simple pore. *In:* Drugs and Transport Processes. B.A. Callingham, Editor. p. 193. University Park Press, Baltimore, London, Tokyo

Hladky, S.B., Harris, I.D. 1967. An ion displacement membrane model. *Biophys. J.* **7**:535

Hladky, S.B., Haydon, D.A. 1970. Discreteness of conductance change in bimolecular lipid membranes in the presence of certain antibiotics. *Nature (London)* **225**:451

Hladky, S.B., Haydon, D.A. 1972. Ion transfer across lipid membranes in the presence of gramicidin A. I. Studies of the unit conductance channel, *Biochim. Biophys. Acta.* **274**:294

Läuger, P. 1973. Ion transport through pores: A rate-theory analysis, *Biochim. Biophys. Acta.* **311**:423

Myers, V.B., Haydon, D.A. 1972. Ion transfer across lipid membranes in the presence of gramicidin A. II. The ion selectivity. *Biochim. Biophys. Acta.* **274**:313

Neher, E. 1975. Ionic specificity of the gramacidin channel and the thallous ion. *Biochim. Biophys. Acta.* **401**:540

Urry, D.W. 1972*a*. Protein conformation in biomembranes: Optical rotation and adsorption of membrane suspensions. *Biochim. Biophys. Acta.* **265**:115

Urry, D.W. 1972*b*. The gramicidin A transmembrane channel: A proposed $\pi_{(L,D)}$ helix. *Proc. Nat. Acad. Sci. USA* **68**:672

Urry, D.W., Goodall, M.C., Glickson, I.D., Mayers, D.C. 1971. The gramicidin A transmembrane channel: Characteristics of head-to-head dimerized $\pi_{(L,D)}$ helices. *Proc. Nat. Acad. Sci. USA* **68**:1907

Veatch, W.R., Fossel, E.T., Blout, E.R. 1974. The conformation of gramicidin A. *Biochemistry* **13**:5249

Woodbury, J.W. 1971. Eyring rate theory model of the current-voltage relationship of ion channels in excitable membranes. *In:* Chemical Dynamics: Papers in Honor of Henry Eyring. J. Hirschfelder, editor. John Wiley and Sons, New York